Pergamon

Geochimica et Cosmochimica Acta, Vol. 66, No. 1, pp. 109–123, 2002

0016-7037/02 $22.00 + .00

PII S0016-7037(01)00754-2

Tracer diffusion of Mg, Ca, Sr, and Ba in Na-aluminosilicate melts

KNUT ROSELIEB[1,2,*] and ALBERT JAMBON[1]

[1]Laboratoire Magie, UMR 7047 CNRS, Université Pierre et Marie Curie, 4 Place Jussieu, F-75252 Paris Cedex 05, France
[2]Mineralogisch-Petrologisches Institut, Universität Göttingen, Goldschmidtstrasse 1, D-37077 Göttingen, Germany

(*Received December* 2, 1999; *accepted in revised form June* 28, 2001)

Abstract—We employed the thin source technique to investigate tracer diffusion of Mg, Ca, Sr, and Ba in glasses and supercooled melts of albite ($NaAlSi_3O_8$) and jadeite ($NaAlSi_2O_6$) compositions. The experiments were conducted at 1 bar and at temperatures between 645 and 1025°C. Typical run durations ranged between 30 min and 35 days. The analysis of the diffusion profiles was performed with the electron microprobe. Diffusivities of Ca, Sr, and Ba were found to be independent of either duration t of the experiment or tracer concentration M, initially introduced into the sample. Mg exhibits a diffusivity depending on run time and concentration and tracer diffusivity is derived by extrapolation to $M/\sqrt{t} = 0$. Temperature dependence of the diffusivity D can be represented by an Arrhenius equation $D = D_o \exp(-E_a/RT)$, yielding the following least-squares fit parameters (with D in m^2/s and E_a in kJ/mol): $D_{Mg} = 1.8 \cdot 10^{-5} \exp(-234 \pm 20/RT)$, $D_{Ca} = 3.5 \cdot 10^{-6} \exp(-159 \pm 6/RT)$, $D_{Sr} = 3.6 \cdot 10^{-6} \exp(-160 \pm 6/RT)$, and $D_{Ba} = 6.0 \cdot 10^{-6} \exp(-188 \pm 12/RT)$ for albite; and $D_{Mg} = 8.3 \cdot 10^{-6} \exp(-207 \pm 18/RT)$, $D_{Ca} = 3.8 \cdot 10^{-6} \exp(-153 \pm 4/RT)$, $D_{Sr} = 2.3 \cdot 10^{-6} \exp(-150 \pm 4/RT)$, and $D_{Ba} = 3.7 \cdot 10^{-5} \exp(-198 \pm 4/RT)$ for jadeite composition. Ca and Sr diffusivities agree within error in both compositions and exhibit the fastest diffusivities, whereas Mg reveals the lowest diffusivity. The relationship between activation energy and radius shows a minimum at Ca and Sr for albite and jadeite compositions extending the relationship already observed elsewhere for alkalies. With increasing substitution of Si by (Na + Al), diffusivities increase, whereas activation energies decrease. Furthermore, a simple model modified from that of Anderson and Stuart (Anderson O. L. and Stuart D. A., "Calculation of activation energy of ionic conductivity in silica glasses by classical methods," *J. Am. Ceram. Soc.* **37,** 573–580, 1954) is discussed for calculating the activation energies. *Copyright © 2002 Elsevier Science Ltd*

1. INTRODUCTION

Knowledge of the diffusion behavior of trace elements in silicate melts is important to understand quantitatively magmatic processes—for example, during crystal growth, trace element partitioning can be influenced by the diffusivity of the trace element in the silicate melt (e.g., Albarède and Bottinga, 1972). In partially molten systems, diffusivities of trace elements in melts are rate-determining in reaching local equilibrium, a prerequisite for the interpretation of isotope signatures of mantle rocks (e.g., Hofmann and Hart, 1978). Melting of solids and magma mixing are also under diffusive control, with a relationship existing between chemical interdiffusion and tracer diffusion (e.g., Zhang et al., 1989).

In view of the complexity of natural magmas, systematic studies as a function of composition are needed to improve our understanding of diffusion properties. Furthermore, such studies, particularly those that include analyses of atoms of different size and charge, provide insight into the dynamics and structure of silicate melts and are necessary to develop quantitative models of diffusion mechanisms.

Glasses and supercooled melts along the join SiO_2-$NaAlSi_2O_6$ are particularly useful because they have a similar tridymite-like structure (Taylor and Brown, 1979) with varying Na contents within the available voids. Hence, introducing small amounts of other trace elements (noble gases, alkalies, alkaline earths) into these matrixes, assuming that they diffuse along similar interring positions and voids, yields potential information on diffusion mechanism in melts of simple composition.

Here, we report complementary measurements to previous works on diffusivities of alkaline earths in the system SiO_2-$NaAlSi_2O_6$ (SiO_2: Ca, Ba: Zhabrev et al., 1976; $NaAlSi_3O_8$: Ca: Jambon and Delbove, 1977; Sr, Ba: Jambon, 1980). Specifically, we present new data on the diffusivity of alkaline earths in albite and jadeite composition glasses and melts, and we present what is to our knowledge the first experimental results of Mg tracer diffusion in highly viscous silicate melts, one of the most abundant cations in the Earth. We performed the experiments at temperatures at which structural relaxation times (Siewert and Rosenhauer, 1994, 1997) are much shorter than the run duration of the diffusion experiments, and therefore diffusivity of alkaline earths is investigated in relaxed melts (cf. Roselieb and Jambon, 1997), with the exception of Ca and Sr diffusivity, which was studied at 645°C and 650°C in albite glass.

At the end of this article, we present a detailed discussion of the diffusion behavior of noble gases, alkalies, and alkaline earths within the framework of a calculation model of activation energies in melts of the system SiO_2-$NaAlSi_2O_6$.

2. EXPERIMENTAL PROCEDURE

The jadeite glass was obtained from Schott-Glaswerke, Mainz, and it is from the same batch used previously for the tracer diffusion measurements of Li (Roselieb et al., 1998) and of K, Rb, and Cs (Roselieb and Jambon, 1997), for measurements of the electrical conductivity of

* Author to whom correspondence should be addressed, at Mineralogisch-Petrologisches Institut, Universität Göttingen, Goldschmidtstrasse 1, D-37077 Göttingen, Germany (kroseli@gwdg.de).

Table 1. Composition of the starting materials (wt%).[a]

Material	SiO_2	Al_2O_3	Na_2O	CaO	MgO	FeO	K_2O	Rb_2O	Cs_2O	MnO
Albite	69.1	19.33	11.74	n.d.	n.d.	n.d.	0.022	<0.02	<0.02	n.d.
Jadeite B5560	59.86	25.52	14.58	0.018	0.004	0.023	0.022	<0.02	<0.02	0.021

[a] Analysis by electron microprobe (jadeite: D. Badia, personal communication). n.d., not determined.

Na (Fritzsche, 1990; Fuchser, 1996), noble gas diffusivity (Roselieb et al., 1995, 1996), noble gas solubility (Walter et al., 2000), and structural relaxation times (Siewert and Rosenhauer, 1994). The albite glass was prepared by D. Dingwell from oxides at the Bayerisches Geoinstitut in Bayreuth. Table 1 summarizes the chemical analyses of the starting glasses. Cuboids with an edge length of 2 mm and height of 3 mm, cubes with an edge length of 1.5 and 2 mm, or cylinders with a height of 3.6 mm and a diameter of 2.6 mm were prepared from the starting glasses.

The thin source enriched with the tracer element was produced by depositing a chloride solution on a polished surface of the glass sample and a subsequent short preannealing in air, except for the Mg samples and some Sr and Ba albite samples, which were annealed in an Ar atmosphere of 1 bar. The run durations and temperatures of this preanneal are summarized in Table 2. The variation of the preanneal time and temperature allows the production of samples with varying amounts of the tracer. The thickness of the produced thin source is roughly one order of magnitude smaller than the length of the diffusion profile, except in case of Sr in albite, where profile lengths are only three to six times larger than the extension of the thin source.

To remove excess salt after the preanneal, the samples were washed with distilled water. This procedure yields a nearly homogeneous thin source. The errors of the measured integral amounts of the introduced tracer, M (see below), from various profile analyses on the same sample are usually smaller than 10%, and only a few samples exhibit errors up to ~45%. However, for Ba and especially Mg, this approach was not successful, and M values differ, sometimes significantly, from one profile to the next for the same sample. This effect presumably results from the formation of refractory alkaline earths oxides, which are insoluble in water. Consequently, we rejected the first set of results for Mg; the samples of subsequent experiments on jadeite and albite for Mg, Ca, Sr, and Ba were washed with a 10% HCl solution after the pretreatment to remove the oxide layer (≥run x.130596; see Tables 3 to 6; the six numbers after the decimal point indicate the date of sample preparation [x.ddmmyy]). This yields a homogeneous thin source of Ba, although tracer concentrations are decreased when compared with samples treated at similar temperatures and durations, but washed with water. For Ca and Sr, no significant differences between both procedures were observed. Results for Ca, Sr, and Ba from both procedures agree within experimental error (Tables 4 to 6).

Mg samples preannealed in air at 720 to 800°C for 10 to 20 min were more affected by washing the samples with HCl. In this case, the treatment with HCl resulted in a nearly complete removal of the tracer deposit, and remaining tracer amounts (100 to 300 ppm) at the top of the polished surface were only slightly above the detection limit of the microprobe, thus resulting in enormous errors for the derived diffusivity. Therefore, only one experiment with albite and two with jadeite exhibited sufficient Mg concentrations to allow reliable measurements of diffusion profiles (cf. Table 3).

Table 2. Run durations t and temperatures T of the preannealing in vitreous albite and jadeite.

Material	Mg	Ca	Sr	Ba
Albite				
T (°C)	740–1020	800	750–900	700–900
t (min)	5–60	5–40	20–60	20–75
Jadeite				
T (°C)	720–950	800	700	700–800
t (min)	10–60	1–5	10–60	60

We interpret this as a removal of thin layers of alkaline earth oxides formed during the pretreatment step (Jambon, 1980; Chakraborty et al., 1994), which were then dissolved and removed. Oxides should also be formed by the other alkaline earths, but their contribution to the source of tracer is most evident for elements with low diffusivities (e.g., Mg and Ba because of a competition between penetration and oxidation at the surface). In the case of Ca and Sr, the influence of the oxide layer is negligible.

To improve the production of an adequate thin source of Mg, we enhanced the temperature of the pretreatment. Furthermore, we performed the preanneal for all Mg experiments and some Sr and Ba experiments on albite glass (Tables 5, 6) under an Ar atmosphere of 1 bar to minimize the formation of oxides. After that, the samples were washed in distilled water. This procedure yields samples with homogeneous sources and measurable amounts of Mg. However, because the Mg diffusion is rather slow, high preanneal temperatures are required to produce a sufficient enrichment of Mg. Additional attempts to enhance the Mg concentration by leaching the glass samples for 10 min in 10% HCl before depositing the salt solution yield enriched Mg concentrations of ~25% for jadeite glass, but for albite, this method had no significant effect. The results of these experiments with Sr and Ba agree within error with those prepared in air (see above).

The diffusion experiments were performed in a 1-bar furnace operated in air. Run temperatures ranged from 645 to 1025°C and were measured with a $Pt_{94}Rh_6$-$Pt_{70}Rh_{30}$ and a Pt_{100}-$Pt_{90}Rh_{10}$ thermocouple for the experiments performed in Paris and Göttingen, respectively (cf. Tables 3 to 6). The temperature was checked against the melting point of Au and NaCl and was believed to be accurate within ±5°C. The duration of the experiments ranged between 30 min and 35 d. Run temperatures were typically reached within 40 s to 5 min, depending on temperature. After the experiment, some samples run at higher temperatures were slightly rounded, but this has no significant effect on the diffusivity because the results from these samples are indistinguishable within error from the results of other experiments.

The subsequent preparation and analysis, which used an electron microprobe CAMECA SX 50, was similar to that previously described by Roselieb and Jambon (1997). Briefly, by use of the K_α lines of Mg and Ca and the L_α lines of Sr and Ba, profiles were collected at operating conditions of 15 kV, beam current of 40 nA (Mg, Ca, Sr) and 50 nA (Mg, Ca, Sr, Ba), and counting times of 30 s (Mg), 10 and 20 s (Ca), 30 and 50 s (Sr) and 30 s (Ba). The beam diameter was between 10 and 15 μm. We checked the stability of the analysis by repeating measurements on the same point (cf. below), and Mg, Ca, Sr, and Ba were found to be stable under these conditions. Typical concentration-distance profiles are presented in Figure 1. The diffusivities were derived from fitting the measured profiles with the corresponding solution for a thin source on top of a semi-infinite cylinder (Crank, 1975):

$$C(x, t) = \frac{M}{\sqrt{\pi Dt}} \exp(-x^2/4Dt) \quad (1)$$

where C(x,t) is the measured concentration of tracer at distance x, M is the amount introduced initially into the sample, D is the diffusivity, and t is the duration of the run. The background concentration was substracted to obtain C from the total measured concentration. Linearizing Eqn. 1 and plotting lnC vs. x^2 yields the diffusivity from the slope $-1/(4Dt)$ and M from the intercept $M/(\pi Dt)^{1/2}$ of a linear least-square regression. Tables 3 to 6 summarize the results for D and M as mean values calculated from various profiles on each sample.

The linear least-square regression usually exhibits a statistical error of ±0.05 log units or less (1σ). Tables 3 to 6 summarize the measure-

Table 3. Results of the tracer diffusion of Mg in vitreous albite and jadeite.[a]

Run	T (°C)	t (s)	log D (D in m^2/s)	1σ	r	M (ppm · m)	1σ	n	log D (D in m^2/s)	Remarks
Albite										
1.300197	800	3,024,000	−15.82	0.1	0.994	0.08	0.015	4		
2.300197	800	3,024,000	−15.63	0.07	0.996	0.13	0.015	4		
3.300197	800	3,024,000	−15.89	0.03	0.997	0.1	0.006	4		
4.300197	800	3,024,000	−15.98	0.07	0.993	0.05	0.011	4		
1.090796	800	3,110,400	−16.14	0.14	0.723	0.01	0.001	6	−16.16 ± 0.07	Air
5.300197	850	1,036,800	−15.01	0.1	0.99	0.23	0.03	4		
6.300197	850	1,036,800	−14.93	0.04	0.994	0.19	0.014	4		
7.300197	850	1,036,800	−15.28	0.04	0.996	0.13	0.008	4		
8.300197	850	1,036,800	−15.25	0.03	0.99	0.1	0.007	4		
19.300197	850	2,124,900	−15.36	0.06	0.998	0.13	0.011	4		
20.300197	850	2,124,900	−14.98	0.06	0.992	0.28	0.017	3		
21.300197	850	2,124,900	−15.32	0.03	0.996	0.11	0.014	4		
22.300197	850	2,124,900	−15.24	0.04	0.995	0.14	0.011	3	−15.52 ± 0.07	
9.300197	900	774,000	−14.69	0.01	0.996	0.18	0.013	4		
10.300197	900	774,000	−14.86	0.05	0.993	0.11	0.01	5		
11.300197	900	774,000	−14.77	0.04	0.992	0.13	0.008	4		
12.300197	900	774,000	−14.8	0.03	0.992	0.13	0.007	3	−15.1 ± 0.05	
9.201296	950	153,000	−14.83	0.15	0.98	0.01	0.002	3		
10.201296	950	153,000	−14.81	0.11	0.951	0.02	0.007	5		
13.201296	950	153,000	−14.25	0.03	0.997	0.13	0.007	4		
14.201296	950	153,000	−14.26	0.03	0.991	0.13	0.004	4		
13.300197	950	442,800	−14.42	0.02	0.996	0.19	0.005	5		
14.300197	950	442,800	−14.47	0.04	0.991	0.16	0.002	3		
15.300197	950	442,800	−14.52	0.06	0.993	0.14	0.01	3	−14.9 ± 0.02	
16.300197	1020	28,800	−13.68	0.08	0.993	0.18	0.011	4		
17.300197	1020	28,800	−13.74	0.07	0.987	0.14	0.013	4		
18.300197	1020	28,800	−13.85	0.04	0.995	0.11	0.013	3	−14.11 ± 0.12	
Jadeite										
1.290197	800	1,638,000	−15.16	0.04	0.999	0.16	0.007	3		
2.290197	800	1,638,000	−14.98	0.01	0.997	0.29	0.005	2		
3.290197	800	1,638,000	−14.93	0.01	0.995	0.39	0.018	2		
4.290197	800	3,024,000	−15.01	0.01	0.995	0.31	0.003	3		
5.290197	800	3,024,000	−14.88	0.02	0.998	0.42	0.014	2	−15.28 ± 0.11	
6.290197	850	687,600	−14.5	0.01	0.998	0.37	0.009	3		
7.290197	850	687,600	−14.49	0.01	0.998	0.41	0.003	2		
19.290197	850	2,124,900	−14.58	0.01	0.997	0.39	0.009	4		
20.290197	850	2,124,900	−14.62	0.02	0.998	0.38	0.012	3		
21.290197	850	2,124,900	−14.53	0.03	0.996	0.38	0.015	3		
22.290197	850	2,124,900	−14.5	0.03	0.998	0.45	0.012	4	−14.66 ± 0.06	
1.201296	900	79,200	−13.91	0.04	0.996	0.38	0.015	4		
3.201296	900	79,200	−13.99	0.06	0.996	0.26	0.061	5		
4.201296	900	79,200	−13.82	0.05	0.991	0.43	0.025	5		
11.290197	900	79,200	−14.15	0.02	0.997	0.13	0.004	3		
12.290197	900	79,200	−13.95	0.03	0.994	0.3	0.005	2		
10.030696	900	82,800	−14.12	0.16	0.775	0.01	0.001	6		Air
8.030696	900	241,200	−14.23	0.08	0.773	0.02	0.002	6		Air
8.290197	900	442,800	−14.18	0.02	0.996	0.37	0.007	3		
9.290197	900	442,800	−14.09	0.01	0.996	0.51	0.014	2		
10.290197	900	442,800	−14.07	0.01	0.997	0.5	0.009	2	−14.23 ± 0.03	
5.201296	950	82,800	−13.59	0.03	0.998	0.46	0.017	3		
6.201296	950	82,800	−13.77	0.07	0.92	0.04	0.005	3		
7.201296	950	82,800	−13.82	0.06	0.997	0.16	0.034	5		
8.201296	950	82,800	−13.67	0.04	0.995	0.34	0.088	5		
13.290197	950	243,000	−13.84	0.01	0.996	0.42	0.022	3		
14.290197	950	243,000	−13.77	0.02	0.991	0.51	0.009	3		
15.290197	950	243,000	−13.78	0.01	0.998	0.53	0.002	4	−13.86 ± 0.06	
16.290197	1020	18,000	−13.26	0.01	0.998	0.35	0.009	4		
17.290197	1020	18,000	−13.2	0.01	0.996	0.43	0.014	3		
18.290197	1020	18,000	−13.18	0.01	0.995	0.4	0.012	3	−13.56 ± 0.25	

[a] T = run temperature; t = run time; D = diffusivity; r = correlation coefficient of the linearized profiles (see text); M = calculated amount of the tracer initially deposited on the sample; n = number of analysed profiles. 1σ error for D represents mean values of the measured profiles on the sample. Last column indicates extrapolated values to $M/\sqrt{t} = 0$ (see text) (error 1σ). All experiments were performed in Göttingen. All runs preannealed in Ar, except those indicated in air.

Table 4. Results of the tracer diffusion of Ca in vitreous albite and jadeite.[a]

Run	T (°C)	t (s)	log D (D in m^2/s)	1σ	r	M (ppm · m)	1σ	n
Albite								
5.040697	650	335,700	−14.53	0.04	0.996	0.31	0.011	6
16.150596	800	32,580	−13.17	0.03	0.993	0.24	0.012	6
4.021296	800	55,860	−13.15	0.03	0.996	0.4	0.012	4
3.021296	900	7,200	−12.41	0.02	0.997	0.36	0.01	4
4.131094	1020	3,600	−12.03	0.11	0.978	0.17	0.024	5
1.040697	1025	2,660	−11.88	0.03	0.994	0.33	0.005	4
2.040697	1025	2,660	−11.83	0.02	0.997	0.49	0.018	4
Jadeite								
7.201294	800	86,400	−12.91	0.02	0.989	0.81	0.007	4
8.201294	800	86,400	−12.89	0.01	0.998	1.72	0.036	2
9.201294	801	255,600	−12.94	0.03	0.995	1.5	0.089	4
15.201294	801	255,600	−12.92	0.02	0.984	1.33	0.039	3
8.150596	900	7,200	−12.26	0.01	0.997	0.53	0.037	4
9.150596	900	7,200	−12.18	0.03	0.998	0.79	0.076	5
10.150596	900	7,200	−12.18	0.01	0.999	0.97	0.066	4
11.201294	900	10,800	−12.25	0.01	0.996	1.32	0.003	2
11.150596	900	32,400	−12.21	0.01	0.997	1.1	0.024	3
12.150596	1020	1,800	−11.65	0.01	0.999	0.61	0.038	4
13.150596	1020	1,800	−11.61	0.02	0.998	0.84	0.089	4
14.150596	1020	1,800	−11.62	0.03	0.996	0.76	0.118	3
5.131094	1020	3,600	−11.67	0.03	0.996	0.69	0.042	2
15.150596	1020	7,200	−11.66	0.02	0.987	0.71	0.039	3

[a] See Table 3. Experiments with run numbers ≥ x.150596 (x.ddmmyy) were performed in Göttingen (see text).

ments of the various profiles on each sample as mean values with a corresponding error, usually ±0.05 log units or less (1σ). The profiles were measured employing various techniques: repeated, overlapping, or obliquely to the interface (cf. Roselieb and Jambon, 1997). An estimate of the overall experimental error is possible from runs performed under identical run conditions, including uncertainties from the temperature measurement, run time, preannealing conditions, orientation of sample and profile, which yields an error of usually ±0.1 log units or less (1σ), except for Mg in albite, which has errors up to ±0.2 log units (1σ).

3. RESULTS

3.1. Dependence of Diffusivities on Introduced Tracer Concentration and Run Duration

Before evaluating the results obtained in this study, it seems useful to comment on the kind of diffusivity determined. In general, we studied the diffusion of a trace element otherwise not present in the starting material, and therefore, it is evident

Table 5. Results of the tracer diffusion of Sr in vitreous albite and jadeite.

Run	T (°C)	t (s)	log D (D in m^2/s)	1σ	r	M (ppm · m)	1σ	n	Remarks
Albite									
9.021296	645	331,200	−14.56	0.04	0.991	0.57	0.006	4	
12.130596	800	32,580	−13.32	0.04	0.987	0.27	0.011	4	
8.021296	800	55,860	−13.16	0.01	0.998	1.65	0.012	4	Ar
7.021296	900	7,200	−12.47	0.05	0.986	0.67	0.006	4	
13.130596	1020	1,800	−11.98	0.02	0.99	0.33	0.03	3	
6.021296	1020	2,700	−11.9	0.05	0.992	1.11	0.139	4	Ar
Jadeite									
4.130596	800	3,600	−12.85	0.03	0.997	0.68	0.035	3	
3.130596	800	7,200	−12.92	0.02	0.998	0.72	0.018	4	
1.130596	800	32,580	−13.01	0.01	0.996	0.53	0.025	3	
2.130596	800	32,580	−12.96	0.01	0.997	0.71	0.022	2	
6.130596	900	3,600	−12.26	0.02	0.995	0.63	0.011	3	
7.130596	900	3,600	−12.25	0.02	0.996	0.72	0.016	4	
8.130596	900	3,600	−12.24	0.01	0.996	0.89	0.029	4	
5.130596	900	14,400	−12.29	0.05	0.986	0.64	0.006	2	
9.130596	1020	1,800	−11.7	0.02	0.997	0.68	0.001	2	
10.130596	1020	1,800	−11.65	0.02	0.996	0.95	0.045	2	
3.090196	1020	3,300	−11.73	0.03	0.972	0.55	0.009	4	
4.090196	1020	3,300	−11.74	0.04	0.969	0.73	0.047	5	
11.130596	1020	7,200	−11.65	0.05	0.993	0.97	0.029	2	

[a] See Table 3. Experiments with run numbers ≥ x.130596 (x.ddmmyy) were performed in Göttingen. Ar refers to preanneal made in 1 bar Ar atmosphere (see text).

Table 6. Results of the tracer diffusion of Ba in vitreous albite and jadeite.[a]

Run	T (°C)	t (s)	log D (D in m^2/s)	1σ	r	M (ppm · m)	1σ	n	Remarks
Albite									
12.130596	800	442,800	−14.47	0.03	0.94	0.12	0.003	4	
14.130596	800	442,800	−14.42	0.08	0.937	0.13	0.008	5	
12.021296	800	450,000	−14.29	0.02	0.998	0.97	0.027	4	Ar
11.021296	900	90,300	−13.46	0.01	0.997	1.08	0.015	4	Ar
13.130596	1020	7,200	−12.99	0.06	0.972	0.12	0.007	4	
10.021296	1020	7,200	−12.78	0.01	0.998	1.19	0.06	3	Ar, a
10.021296	1020	7,200	−12.73	0.01	0.997	0.76	0.232	3	Ar, b
Jadeite									
3.130596	800	223,200	−14.1	0.01	0.997	0.74	0.007	3	
4.130596	800	223,200	−14.13	0.04	0.989	0.29	0.01	4	
10.130596	800	223,200	−14.09	0.02	0.976	0.3	0.014	3	
1.130596	800	442,800	−14.06	0.07	0.991	0.48	0.026	3	
2.130596	800	442,800	−14.13	0.15	0.874	0.13	0.012	4	
7.130596	900	28,800	−13.24	0.01	0.968	0.21	0.016	4	
15.090196	900	79,200	−13.23	0.02	0.982	0.42	0.016	4	
16.090196	900	79,200	−13.23	0.03	0.979	1.28	0.141	4	
13.090196	901	232,980	−13.09	0.08	0.787	0.28	0.011	3	
11.090196	1020	3,300	−12.4	0.02	0.997	0.43	0.025	4	
12.090196	1020	3,300	−12.41	0.04	0.972	0.21	0.078	4	
8.130596	1020	7,200	−12.54	0.15	0.939	0.15	0.006	3	
9.130596	1020	7,200	−12.44	0.04	0.99	0.57	0.028	3	
11.130596	1020	7,200	−12.51	0.01	0.917	0.15	0.006	3	
9.090196	1020	29,340	−12.38	0.07	0.98	0.41	0.008	2	
10.090196	1020	29,340	−12.49	0.01	0.993	0.95	0.434	2	

[a] See Table 3. Experiments with run numbers ≥ x.130596 (x.ddmmyy) were performed in Göttingen. Ar refers to preanneal made in 1 bar Ar atmosphere (see text); sample 10.021296 was pretreated incidentally with Ba both on the top (a) and on the bottom (b).

that this diffusion process involves some exchange with other cations (here, Na) and is not self-diffusion. Chemical diffusion prevails when strong coupling occurs in the cross-transfer of a number of elements, which is not the case here. When the major cations of the matrix can diffuse rapidly (e.g., Na) there will be on average many more jumps than necessary to balance the flux of a cation of slower or equal diffusivity but in trace amount. In this case, the diffusivity of a tracer will not be limited by the counterflux of major cations; therefore, different tracers will exhibit different diffusivities. With increasing concentration, this may no longer be true, and therefore, this aspect must be considered eventually. Wei and Wuensch (1976) pointed out that low tracer concentrations in the *final* profiles do not preclude concentration-dependent diffusivity. They showed that high solute concentrations, in the early stage of the experiment, could affect the profile significantly, especially for shallow diffusion penetrations (i.e., Mg in our case), depending on the thickness of the thin source and the tracer concentration.

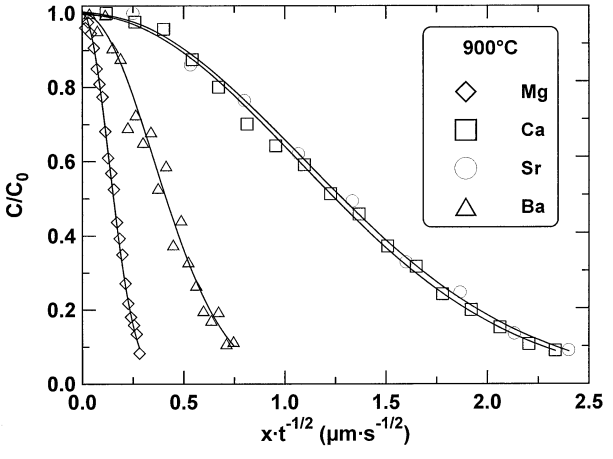

Fig. 1. Diffusion profiles of Mg, Ca, Sr, and Ba in a supercooled jadeite melt at 900°C and run times of 123, 2, 1, and 22 h, respectively. To account for different run times and diffusivities, the distance x is normalized to the run time ($t^{1/2}$). The corresponding concentrations C_o are ~4600, 5100, 11300, and 3500 ppm for Mg, Ca, Sr, and Ba, respectively. Symbols represent analyzed points by electron microprobe, and the solid line indicates the calculated diffusion profile using Eqn. 1 (see text), yielding log D ± 1σ (D in m^2/s) of −14.07 ± 0.01, −12.25 ± 0.01, −12.23 ± 0.01, and −13.21 ± 0.02 for Mg, Ca, Sr, and Ba, respectively.

To investigate the effect of concentration at the beginning of the experiment, we varied our preanneal conditions to produce thin sources of different thickness and the durations of the diffusion experiments. This approach requires measurable concentrations with regard to the sensitivity of the microprobe; because spot sizes of 10 to 15 μm are required, profiles shorter than 30 to 40 μm were impracticable to measure. Besides the problem of introducing adequate tracer concentrations (see above), long durations flatten the concentration gradient and sometimes deteriorate sample geometry due to lowered viscosity. On the other hand, short runs with shallow profiles and high concentrations may be falsified by a concentration-dependent diffusivity in the early stage of the experiment.

Figure 2 presents representative diffusivities of Ca, Sr (at 900°C), and Ba (at 1020°C) in a supercooled jadeite melt as a function of M. For all of these cations, the diffusivity is

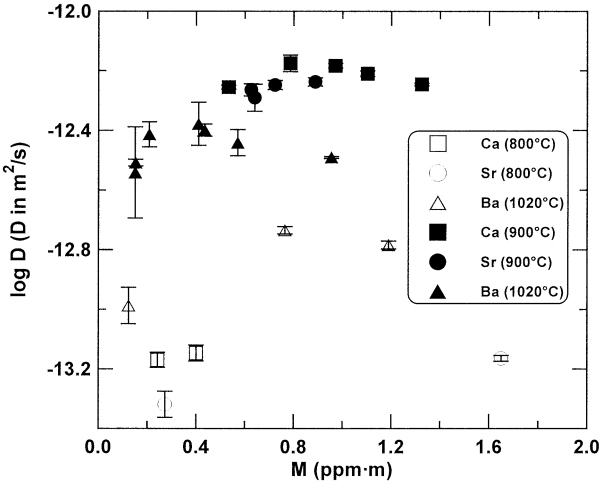

Fig. 2. Diffusivity of Ca, Sr, and Ba in a supercooled jadeite (solid symbols) and albite melt (open symbols) at the indicated temperature as a function of the tracer concentration M (see text). 1σ error bars are obtained from the fit of the diffusion profile.

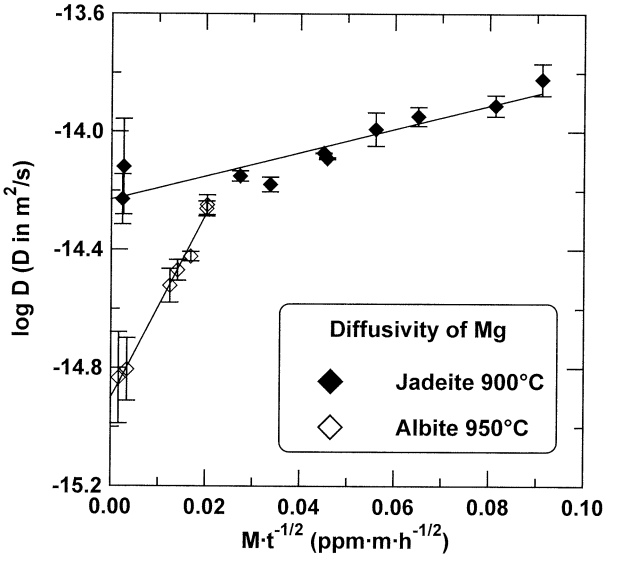

Fig. 3. Diffusivity of Mg in supercooled albite and jadeite melt at the indicated temperature as a function of the tracer concentration M, normalized to $t^{1/2}$ (see text). 1σ error bars are obtained from the mean values of all profiles on each sample. A linear extrapolation to the diffusivity at M = 0 (i.e., infinite dilution), and t = ∞ yields a log D (D in m^2/s) of -14.9 ± 0.02 for $NaAlSi_3O_8$ and -14.23 ± 0.03 for $NaAlSi_2O_6$.

independent on M within the error. We conclude that the derived diffusivity is independent of the introduced concentration of the tracer and run time, and that the tracer diffusivities of Ca, Sr, and Ba in jadeite composition are true tracer diffusivities.

For albite, only a few measurements are available (Fig. 2), and the database are too sparse to demonstrate explicitly that diffusivities are independent of the preanneal conditions. However, the results agree within a range of ~0.2 log units or less, and because the introduced amount of the tracer is comparable to that on jadeite composition, we conclude that the derived diffusivities are true tracer diffusivities as well. This assumption is further supported by the fair agreement between the derived diffusivities of Ca, Sr, and Ba from the radiotracer techniques of Jambon and Delbove (1977) and Jambon (1980) when compared with those from microprobe profiling (this study; see below). It is worth noting that Jambon (1980) gives Sr diffusivities of ±15% in investigations where tracer surface concentration vary by a factor of 300.

Unlike other cations, Mg in both albite and jadeite compositions exhibits a clear dependence of its diffusivity on the amount M of tracer introduced (Fig. 3). Within the attainable M range, the diffusivity increases with increasing M of ~ 0.4 and 0.6 log units for jadeite and albite composition, respectively, which is well above the error range of repeated profiles on the same sample (see above). Furthermore, the diffusivity decreases with increasing run time for a given range of M, yielding diffusivities close to those runs with shorter run times but lower tracer concentrations (Fig. 3). We interpret this as a result of a concentration-dependent diffusion coefficient in the early stage of the experiment (Wei and Wuensch, 1976; cf. above). Therefore, we plotted the diffusivities for each temperature vs. the ratio $M/\sqrt{t}$, as illustrated in Figure 3 for $NaAlSi_2O_6$ (900°C) and $NaAlSi_3O_8$ (950°C), and determined the infinite dilution diffusivity from a linear extrapolation to $M/\sqrt{t} = 0$. The extrapolated values for these tracer diffusivities are listed in Table 3.

Generally, the determined diffusivities should be independent of run duration if no other transport mechanisms are effective (e.g., viscous flow). Experiments on the Ca, Sr, and Ba diffusion in jadeite melt were performed with various run durations, clearly demonstrating that the derived diffusivities do not depend on duration (Tables 4 to 6). In the case of the Mg diffusion, the effect of run time is more evident (Fig. 3), and we interpret this effect as a result of concentration-dependent diffusivity in the early stage of the experiment (see above), rather than from other transport mechanisms other than diffusion. Because the durations are large in comparison with the time for heating up and cooling down the samples, we ignored this contribution, considering the error to be negligible.

3.2. Comparison with Radiotracer Technique

The diffusion measurements of Ca, Sr, and Ba on albite composition were performed to compare our microprobe profiling results (Tables 4 to 6, Fig. 4) with those of the residual activity method of Jambon and Delbove (1977) and Jambon (1980). This allows the comparison of tracer diffusion experiments employing different concentrations of the tracer ($4 \cdot 10^{-5}$ to 10^{-2} ppm · m) compared with 0.12 to 1.65 ppm · m for the microprobe profiling and similar depths of penetration. Results for Ba (Fig. 4) are in good agreement within the investigated temperature range, whereas Ca and Sr diffusivities derived from microprobe profiling are ~0.4 to 0.7 and ~0.2 to 0.7 log units, respectively, higher than those from the radiotracer technique. Jambon (1980) studied the diffusion of Sr in albite glass at 697°C and with concentrations of the tracer from $4 \cdot 10^{-5}$ to 10^{-2} ppm · m. He reports a reproducibility within ±15% (four samples and a single run) with a profile length of ~30 μm

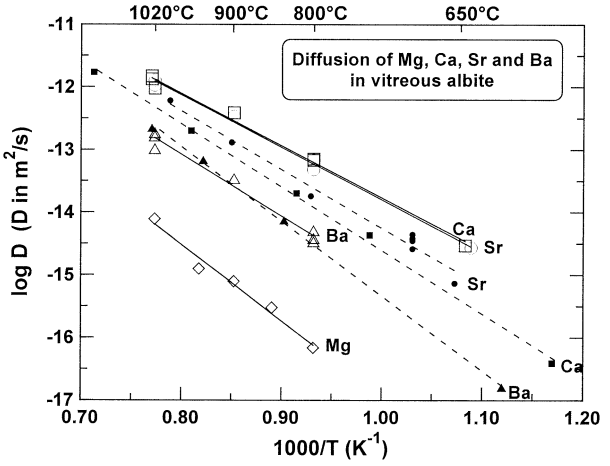

Fig. 4. Arrhenius diagram of the Mg, Ca, Sr, and Ba diffusivity in vitreous albite. Symbols indicate the diffusivity derived from mean values on each sample (Ca, Sr, Ba) and extrapolated values to $M/t^{1/2} = 0$ (Mg) (cf. Tables 3 to 6). Error bars are usually within the symbol size and are omitted for clarity. The solid line represents a fit with an Arrhenius equation. Results for diffusivities from the radiotracer technique for Ca (Jambon and Delbove, 1977) and Sr, Ba (Jambon, 1980) are indicated by filled symbols and the Arrhenius fit by dashed lines.

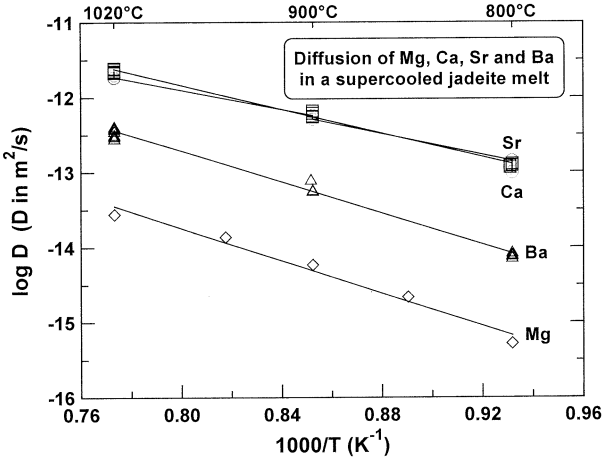

Fig. 5. Arrhenius diagram of the Mg, Ca, Sr, and Ba diffusivity in a supercooled jadeite melt. Symbols indicate the diffusivity derived from mean values on each sample (Ca, Sr, Ba) and extrapolated values to $M/t^{1/2} = 0$ (Mg) (cf. Tables 3 to 6). Error bars are usually within the symbol size and are omitted for clarity. The solid line represents a fit with an Arrhenius equation.

yielding log D (D in m^2/s) of -14.45 ± 0.1. This can be compared with the present results obtained from an Arrhenius fit to the data of log D (D in m^2/s) of -14.06 ± 0.6. Both results agree within experimental error, and we conclude that no evidence of concentration dependence exists in the case of Sr. The deviations between the results of Jambon (1980) and ours probably results from a small difference in the starting material, slightly different experimental procedures, or both.

Activation energies derived from the diffusivities of the microprobe profiling are ~20% lower when compared with those from the radiotracer technique (see below; Figs. 4, 7). This fair agreement demonstrates that the microprobe technique is not significantly falsified by the concentration dependent diffusion during the early stage of the experiment.

3.3. Temperature Dependence

To determine the temperature dependence, we used the mean values of the average diffusivities obtained from the measured profiles on each sample for Ca, Sr, and Ba and extrapolated values to $M/t^{1/2} = 0$ for Mg (summarized in Tables 3 to 6). They are plotted in Figures 4 and 5 for albite and jadeite, respectively, against reciprocal temperature. The solid line represents a linear fit of the data according to an Arrhenian equation,

$$D = D_o \exp\left(-\frac{E_a}{RT}\right) \quad (2)$$

Herein, D is the diffusivity at temperature T, D_o (m^2/s) the preexponential factor, E_a (J/mol) the activation energy, and R the gas constant. For all alkaline earth cations, a clear Arrhenian behavior is observed, and values for E_a and D_o are summarized in Table 7 for albite and jadeite. For both Ca and Sr diffusion in albite, one experiment was performed below the glass transition temperature Tg—that is, at viscosities greater than 10^{12} Pa · s. Results from both glass and supercooled liquid can be well described by a single Arrhenian expression, indicating no significant influence of the glass transition on the tracer diffusivities, as found in previous measurements for Ca, Sr, and Ba in vitreous albite (Jambon and Delbove, 1977; Jambon, 1980; cf. Fig. 4).

3.4. Diffusivity and Activation Energy of Alkaline Earths in the System SiO_2-$NaAlSi_2O_6$

Ca and Sr exhibit maximum diffusivities in both $NaAlSi_3O_8$ and $NaAlSi_2O_6$, whereas Mg, the smallest cation investigated, shows the lowest diffusivity (Figs. 4, 5). A similar observation is made for alkalies—for example, in vitreous obsidian (Jambon, 1983) or jadeite (Roselieb et al., 1998)—where a maximum diffusivity is exhibited for a cation of intermediate size (Na). The effect of matrix composition is presented in Figure 6 at a constant temperature of 900°C and includes data from the radiotracer technique. In contrast to the observed behavior of alkalies in vitreous albite and jadeite (cf. Roselieb and Jambon, 1997), where diffusivities are indistinguishable within experi-

Table 7. Arrhenius parameters D_0 and E_a between temperatures T_{min} and T_{max} of Mg, Ca, Sr, and Ba diffusion in albite and jadeite melts.

Melt	log D_0 (D_0 in m^2/s)	$\pm 1\sigma$	E_a (kJ/mol)	$\pm 1\sigma$	T_{min} (°C)	T_{max} (°C)
Albite						
Mg	−4.75	0.89	234	20	800	1020
Ca	−5.46	0.3	159	6	650	1025
Sr	−5.44	0.28	160	6	645	1020
Ba	−5.22	0.52	188	12	800	1020
Jadeite						
Mg	−5.08	0.79	207	18	800	1020
Ca	−5.42	0.16	153	4	800	1020
Sr	−5.63	0.19	150	4	800	1020
Ba	−4.43	0.2	198	4	800	1020

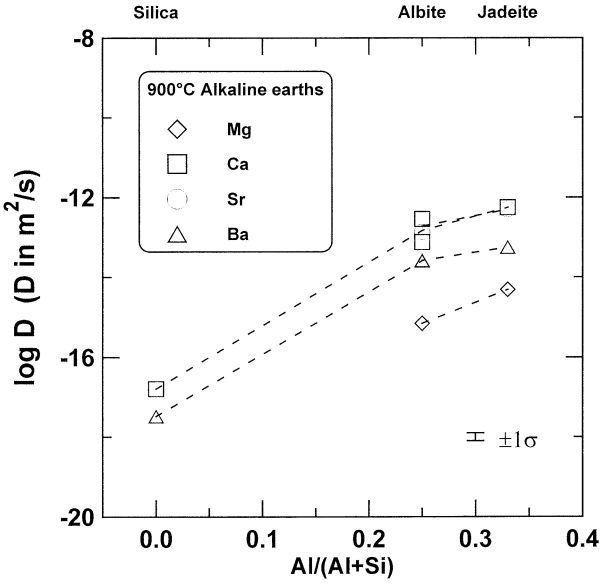

Fig. 6. Diffusivities of alkaline earths as a function of the Al/(Al + Si) ratio. For data sources, see Figures 4 and 5.

mental error, the diffusivity of alkaline earths increases with increasing (Na + Al)/Si content, clearly evident from SiO_2 to $NaAlSi_3O_8$. With increasing Na content toward $NaAlSi_2O_6$, diffusivities further increase for Mg, whereas Ca, Sr, and Ba diffusivities in both aluminosilicate compositions are rather similar.

In Figure 7, the activation energy as a function of diffusing species radius is presented. For albite and jadeite compositions, a clear minimum corresponding to a radius of ~1 to 1.2 Å is

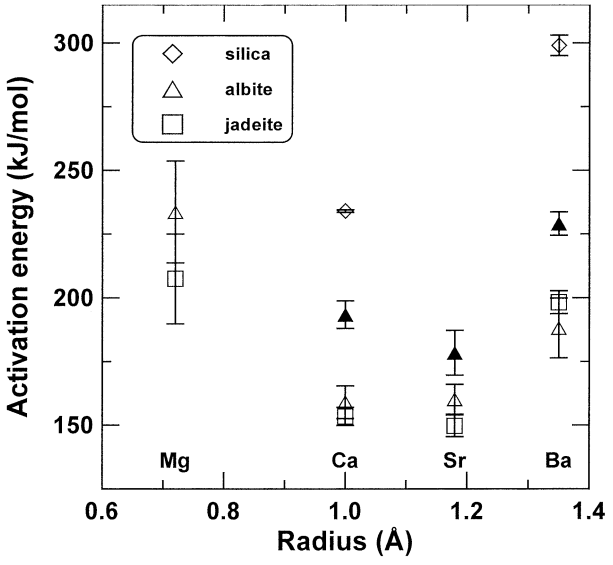

Fig. 7. Activation energies (error bars $\pm 1\sigma$) of alkaline earths in vitreous silica, albite, and jadeite. For albite composition, the solid symbols represent data from the radiotracer technique (cf. Fig. 4). Ionic radii from Shannon (1976). Data source: this study (Table 7); for vitreous silica: Ca, Ba: Zhabrev et al. (1976); vitreous albite: Ca: Jambon and Delbove (1977); Sr, Ba: Jambon (1980).

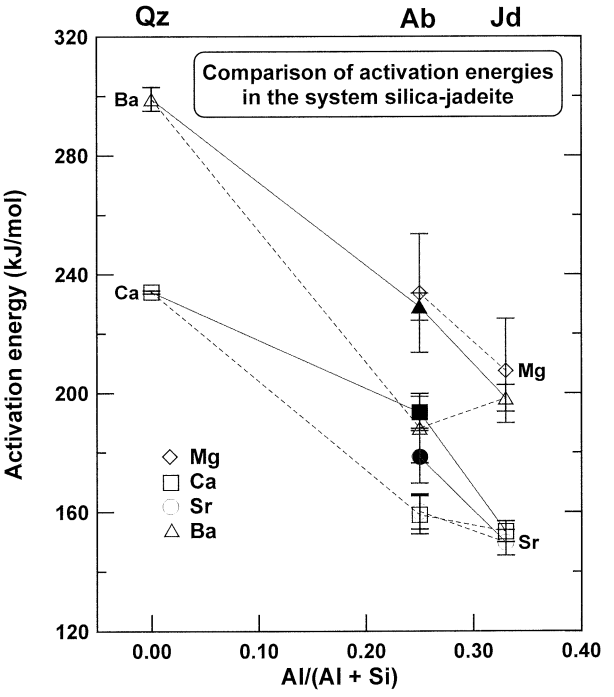

Fig. 8. Activation energies (error bars $\pm 1\sigma$) of alkaline earths as a function of the Al/(Al + Si) ratio. For data sources, see Figure 7. For albite composition, the solid symbols represent data from the radiotracer technique (cf. Fig. 4). The dashed and solid lines indicate the trend including only the albite data from this study and the radiotracer technique, respectively.

evident. For vitreous silica, there are no data for Mg and Sr available, but Ca shows a significantly lower activation energy than Ba, in agreement with the observed behavior in the Na-aluminosilicate compositions. A minimum in the relationship between cation radius and activation energy was previously observed for alkalies at ~1 Å in vitreous obsidian (Jambon, 1983), silica, albite (Roselieb and Jambon, 1997), and jadeite (Roselieb et al., 1998). This minimum can be explained qualitatively with the elastic and electrostatic contributions to the activation energy described in the models presented below. The significance of the activation energy on the diffusivity emerges clearly from a comparison with the observed maximum in the diffusivity of Ca and Sr (Figs. 4 to 6), indicating that the cations with the smallest activation energy exhibit the highest probability for a diffusive jump.

3.5. Activation Energy of Alkaline Earths as a Function of Composition

Figure 8 compares mean values of all available data for the activation energy of diffusion for alkaline earths in the system SiO_2-$NaAlSi_2O_6$, including data from this study as well as from the radiotracer technique (Jambon and Delbove, 1977; Jambon, 1980). For Mg, Ca, and Sr the activation energy clearly decreases with increasing substitution of Si by (Na + Al). However, for Ba, some discrepancy between both studies exists despite excellent agreement of the results between 800 and 1020°C (cf. Fig. 4) and differences in the activation energies due to only one measurement in the glass at 620°C (Jambon,

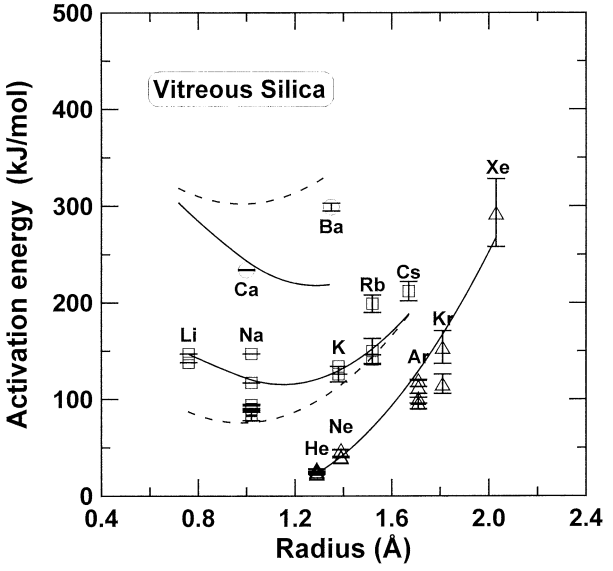

Fig. 9. Activation energies (error bars $\pm 1\sigma$) of noble gases, alkalies, and alkaline earths as a function of particle radius in vitreous silica. For symbols without error bars, either there are no error estimates available or they are within the symbol size. Solid lines and dashed lines represent the best fit employing Eqns. 9 and 11, respectively (see text). Data sources: He: Swets et al. (1961), Perkins and Begeal (1971), Shelby (1971, 1972); Ne: Frank et al. (1961), Perkins and Begeal (1971), Wortman and Shackelford (1990); Ar: Perkins and Begeal (1971), Nakayama and Shackelford (1990), Carroll and Stolper (1991), Roselieb et al. (1995); Kr: Carroll et al. (1993), Roselieb et al. (1995); Xe: Roselieb et al. (1995); Li: Doremus (1969); Na: Doremus (1969), Frischat (1970), Zhabrev et al. (1976); K: Doremus (1969), Rothman et al. (1982); Rb, Cs: Rothman et al. (1982); Ca, Ba: Zhabrev et al. (1976). Ionic radii from Shannon (1976); noble gas radii from Hirschfelder et al. (1954).

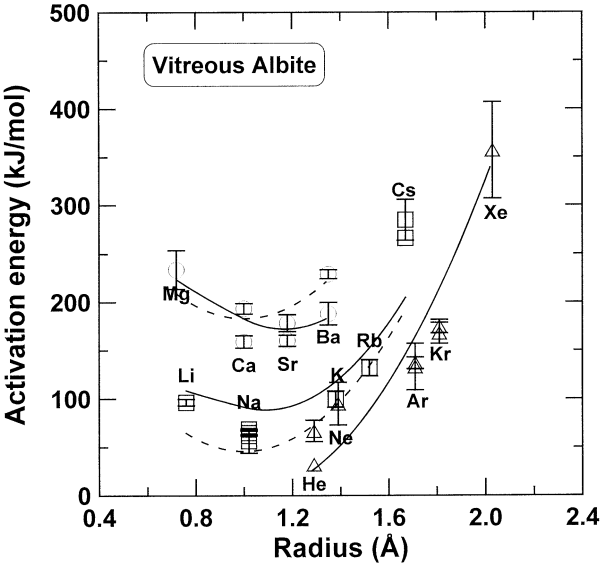

Fig. 10. Activation energies (error bars $\pm 1\sigma$) of noble gases, alkalies, and alkaline earths as a function of particle radius in vitreous albite. Data sources: He: Shelby and Eagan (1976), Roselieb et al. (1992); Ne: Roselieb et al. (1992); Ar: Carroll (1991), Roselieb et al. (1992); Kr: Roselieb et al. (1992), Carroll et al. (1993); Xe: Roselieb et al. (1995); Li: Jambon and Semet (1978); Na: Carron (1969), Jambon and Carron (1976), Fritzsche (1990), Fuchser (1996); K, Rb: Jambon and Carron (1976); Cs: Jambon and Carron (1976), Roselieb and Jambon (1997); Mg: this work; Ca: Jambon and Delbove (1977), this work; Sr, Ba: Jambon (1980), this work. Compare Figure 9.

1980), resulting in a higher activation energy. If only measurements in the supercooled melt region are considered, a possibly minimum in the activation energy for Ba at $NaAlSi_3O_8$ composition is indicated.

4. DISCUSSION OF MODELS FOR CALCULATING THE ACTIVATION ENERGY OF DIFFUSION

At this stage, it seems that looking for a general formalism for estimating activation energies of diffusion in the system SiO_2-$NaAlSi_2O_6$ is necessary. Anderson and Stuart (1954) first developed a model for calculating activation energies for ionic conductivity in silica glass. This model is discussed in the literature with different points of view (e.g., Jambon, 1982; McElfresh and Howitt, 1986; see below), but to our knowledge, it has never been applied to experimental data that included particles of different size and charge.

For glasses and supercooled melts along the join SiO_2-$NaAlSi_2O_6$, a nearly complete data set of diffusivity measurements for noble gases, alkalies, and alkaline earths is available (see captions to Figs. 9 to 11 for references). They are derived from both electrical conductivity and tracer diffusion measurements, as well as from permeation measurements of He for $NaAlSi_3O_8$ and $NaAlSi_2O_6$ composition (Shelby and Eagan, 1976). Figures 9 to 11 summarize the available activation energies for particles of different charge and size as a function of radius along the join SiO_2-$NaAlSi_2O_6$. Because few diffusion data are available, especially for He in $NaAlSi_3O_8$ and $NaAlSi_2O_6$, we include the activation energy of permeation for

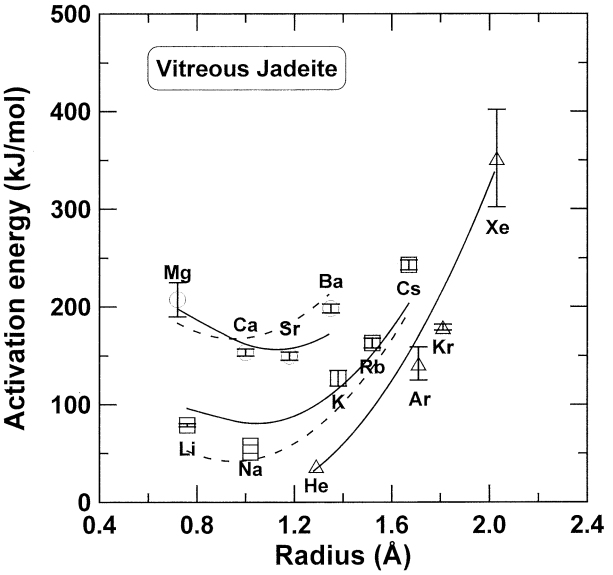

Fig. 11. Activation energies (error bars $\pm 1\sigma$) of noble gases, alkalies, and alkaline earths as a function of particle radius in vitreous jadeite. Data sources: He: Shelby and Eagan (1976); Ar, Kr, Xe: Roselieb et al. (1995); Li: Roselieb et al. (1998); Na: Fritzsche (1990), Fuchser (1996); K, Rb, Cs: Roselieb and Jambon (1997); Mg, Ca, Sr, Ba: this work. Compare Figure 9.

He in albite and jadeite glass (Shelby and Eagan, 1976), and it should be noted that they can be different from that for diffusion, depending on the temperature dependence of solubility.

The following trends emerge from all compositions (Figs. 9 to 11). The activation energy varies with size and charge of the diffusing particle, as follows: an increase with size is conspicuous for noble gases and alkalies whose size varies most. For cations, a minimum is observed corresponding to an ionic radius of ~1 Å. This is especially noticeable for alkaline earths in albite and jadeite compositions.

We now present the model proposed by Anderson and Stuart (1954), including suggestions from the literature for the modification of this model. Furthermore, we propose an alternative formulation of this model derived from our experimental observations. We use the experimental data to assess the parameters of both models and to discuss the derived estimates for the material properties, as well as to decide what model yields a better representation of the data.

4.1. Modified Anderson-Stuart Model

4.1.1. Contributions to the Energy of Activation

We now discuss the various contributions to the activation energy. Anderson and Stuart (1954) first proposed a model (hereafter referred as the Anderson-Stuart model) to calculate the activation energy for the ionic conductivity in silica glass as a function of charge and radius. Two major contributions were considered, the first of which, E_s, is the strain energy required to enlarge the interstice the particle has to jump through. The second contribution for charged particles is the so-called coulombic contribution, E_c. Jambon (1982) argued that a third term to account for defect formation, E_f, is also necessary. Hence, the activation energy E_a can be described as

$$E_a = E_s + E_c + E_f \tag{3}$$

We shall now consider these contributions successively.

4.1.2. Strain Energy

The strain energy, E_s, required on jumping is the energy necessary to dilate the network to enlarge a cavity with a radius r_d, the so-called doorway radius, to the radius r of the diffusing particle. Frenkel (1946) first derived an equation describing the enlargement of a spherical cavity for a close-packed liquid:

$$E_s = 8\pi G r_d N (r - r_d)^2 \tag{4}$$

where G is the shear modulus and N is Avogadro's constant. Anderson and Stuart (1954) modified this equation for a less densely packed glass by halving the constant:

$$E_s = 4\pi G r_d N (r - r_d)^2 \tag{5}$$

Both equations were criticized by McElfresh and Howitt (1986), who argued that describing the enlargement of a spherical cavity yields physically unreasonable results because the activation energy "to enlarge a small cavity can be less than that to enlarge a larger cavity to the same size" (McElfresh and Howitt, 1986, p. 237). Therefore, McElfresh and Howitt (1986) described the diffusive jump as the enlargement of a circular hole over its entire width δW with no variation of the strain in the direction of the width,

$$E_s = \delta W\ \pi G N (r - r_d)^2 \tag{6}$$

where δW is the width and r_d the radius of the cylindrical hole. Because the dilation of the opening passes a maximum, the dilation over the jump distance λ can be described as a sinusoid between 0 and π:

$$E_s = \frac{\lambda}{2}\pi G N (r - r_d)^2 \tag{7}$$

However, despite the differences in the constant, the square root relationship between activation energy and radius of the diffusing particle remains unchanged.

4.1.3. Electrostatic Energy

If charged particles are considered, we must account for the electrostatic energy associated with jumping. The Anderson-Stuart model suggests that the bonding energy between the cation and the surrounding network consists of a Coulomb term of the form

$$E_c = \frac{N}{4\pi\varepsilon_0}\frac{z z_0 e^2}{\varepsilon}\left[\frac{1}{(r + r_0)} - \frac{1}{\lambda/2}\right] \tag{8}$$

Here, N is Avogadro's constant, ε_0 is the dielectric constant of the vacuum, z and z_o represent the charge, r and r_o represent the radius of the cation and oxygen, respectively, e is the charge of the electron, λ is the jump distance, and ε is the dielectric constant.

4.1.4. Energy of Defect Formation

Jambon (1982) first suggested introduction of an energy term E_f for the formation of an available site in the Anderson-Stuart formulation. This kind of contribution is a classical one for diffusion in solids because it is well known that defects (e.g., vacancies) have a strong influence on diffusivities. In the case of melts and glasses, the concept of defects is difficult to define in the same way as in crystals, and it is anticipated that plenty of sites are available for jumping. Still, an energy of formation of available sites is necessary if the creation of sites appropriate for jumping is an activated process. Thermal expansion measurements of glasses clearly show that it not only results from increased vibrations of the atoms (anharmonic oscillations), but it also results from an increase of the free volume.

It is easiest to derive E_f from noble gas data because the electrostatic contribution is zero. However, the determination of E_f depends critically on the choice of the noble gas radii and therefore r_d and λ too (see below).

4.1.5. Modified Anderson-Stuart Model

Anderson and Stuart (1954) calculated the activation energy for different cations in silica glass by combining Eqns. 5 and 8. In view of the criticism of McElfresh and Howitt (1986) with regard to the dilation energy, we prefer the model for the enlargement of a cylindrical cavity (Eqn. 7). Hence, to model the activation energy, we substitute into Eqn. 3 the Eqns. 7 and 8:

$$E_a = \frac{\lambda}{2}\pi GN\,(r - r_d)^2 + \frac{N}{4\pi\varepsilon_0}\frac{zz_0e^2}{\varepsilon}\left[\frac{1}{(r + r_0)} - \frac{2}{\lambda}\right] + E_f \tag{9}$$

This equation has not been previously applied to experimental results. Now it can be tested by using the nearly complete data set of diffusivities of noble gases, alkalies, and alkaline earths in the system SiO_2-$NaAlSi_2O_6$.

4.1.6. Alternative Approach

Considering cations of similar size—for example, the two smallest cations Li and Mg, or Na and Ca—their E_s value is nearly zero, and E_f is only a small fraction of E_a ($<\sim$30 kJ/mol; see Figs. 9 to 11); therefore, E_a should be close to E_c. We obtain from Figures 9 to 11 the following:

$$E_c\,(Mg) >> 2\,E_c(Li) \text{ and } E_c\,(Ca) >> 2\,E_c(Na).$$

This relationship shows that the zz_0 term is not appropriate. We must therefore conclude that Eqn. 8 is not a reasonable model of E_c. This had already been implicitly noticed by Jambon and Delbove (1977) and Jambon (1982) in their analyses of feldspar glasses and obsidian; they preferred a quadratic relationship between E_a and charge for cations of small size ($E_s \approx 0$).

In Figures 9 to 11, we suggest that E_c is independent of the size of the diffusing cation, but a quadratic (or nearly so) relationship with z is given. If we now consider that the charges involved in Eqn. 8 are those of the cation on one hand and of the site on the other (not that of oxygen), then z and z_o are likely to have the same value, but with opposite sign. In other words, a cation resides only in sites of appropriate charge. If we consider that it may jump into a site having a different charge, the surrounding cations should move rapidly to suppress the local charge imbalance. This is possible because sodium, the most abundant cation, is also the most mobile one. We still have a problem with the size dependence in Eqn. 8, even after consideration of the appropriate charge. In the modified Anderson-Stuart formulation, E_c is calculated for a negative charge at a distance varying from $(r + r_o)$ in a regular site to $(\lambda/2)$ in the doorway, which assumes that the site is neutral and the doorway charged in a nonsymmetrical way. If instead we consider that the site carries a charge z_o, compensated by that of the cation and that the doorway is neutral (because of symmetry), then the electrostatic term must be modified. When a charge is located inside a spherical shell of opposite charge, it undergoes no force, no matter what its exact position. If jumping out of the shell, the electrostatic force appears when it reaches its boundary at $\lambda/2$ until it reaches a new stable position at λ. Then E_c becomes

$$E_c = \frac{N}{4\pi\varepsilon_0}\frac{z^2\,e^2}{\varepsilon\lambda} \tag{10}$$

Beside this, the dependence on size can be fully accounted by E_s (as formulated in Eqn. 7), provided that the dependence is still valid for $r < r_d$. The size of r_d, equivalent to the radius of sodium, in these Na-aluminosilicates also suggests that the contribution has to do with the best size for occupying sites. The effect for $r < r_d$ on E_s can be understood as resulting from the distortion of the lattice around a small cation. The similarity between E_s and the energy involved in calculating partition coefficients (Blundy and Wood, 1994) is striking and is a good argument in favor of a similar description.

Hence, the alternative formulation of the coulombic term in the Anderson-Stuart model as required by the experimental results yields for Eqn. 3

$$E_a = \frac{\lambda}{2}\pi GN\,(r - r_d)^2 + \frac{N}{4\pi\varepsilon_0}\frac{z^2\,e^2}{\varepsilon\lambda} + E_f \tag{11}$$

4.2. Constraints on Input Parameters

The application of Eqns. 9 and 11 to model the activation energy requires knowledge of two material properties (G, ε) and two structural parameters (λ, r_d) besides E_f. Although some specific material parameters are known from the literature, it is not evident that these bulk properties are applicable to jumps involving short-range properties. For the sake of simplicity, we shall assume that they do not change with charge or size.

Because it is not possible to obtain a meaningful fit with unique solutions to the five unknown parameters, which depend on each other, it is necessary to fix some parameters.

For diffusion of uncharged particles such as noble gases in vitreous materials, the square root relationship between activation energy and radius (Eqns. 4 to 7) has been confirmed experimentally by various authors (e.g., Perkins and Begeal, 1971; Roselieb et al., 1992, 1995). Employing the equations derived by Frenkel (1946) and Anderson and Stuart (1954), Roselieb et al. (1995) estimated values for the shear modulus

Table 8. Fitted parameters (λ, ε) and fixed parameters (G, r_d, E_f) for calculation of the activation energies of diffusion with Eqns. 9 and 11.[a]

	SiO_2		$NaAlSi_3O_8$		$NaAlSi_2O_6$	
Variable	Eqn. 9	Eqn. 11	Eqn. 9	Eqn. 11	Eqn. 9	Eqn.11
Fit parameters						
λ (Å) $\pm$ 1σ	10.4 $\pm$ 0.6	10.1 $\pm$ 0.7	12.1 $\pm$ 0.7	12.1 $\pm$ 0.8	11.6 $\pm$ 0.6	11.6 $\pm$ 0.7
ε $\pm$ 1σ	5.3 $\pm$ 0.4	1.8 $\pm$ 0.1	7.9 $\pm$ 0.8	2.5 $\pm$ 0.2	8.7 $\pm$ 0.9	2.9 $\pm$ 0.3
Fixed parameters						
E_f (kJ/mol)	0	0	0	0	0	0
G (kbar)	246	246	284	284	269	269
r_d (Å) $\pm$ 1σ	0.98 + 0.32/−0.26	0.98 + 0.32/−0.26	1.0 + 0.4/−0.3	1.0 + 0.4/−0.3	0.95 + 0.35/−0.28	0.95 + 0.35/−0.28
1σ (kJ/mol)	25.6	30.2	32.8	35	22.8	27

[a] G = shear modulus; r_d = doorway radius; E_f = energy of formation; λ = jump length; ε = dielectric constant. Last row indicates 1σ standard deviation between measured and calculated activation energies.

(Table 8), and these are generally in reasonable agreement with bulk values—for example, 313 kbar in silica glass (Bansal and Doremus, 1986) or 50 to 420 kbar in silicate melts (Dingwell and Webb, 1989). Because no bulk values for albite and jadeite composition are available, we used the values given by Roselieb et al. (1995) for supercooled melts in the system SiO_2-$NaAlSi_2O_6$ as fixed parameters (Table 8) as the best estimation for a shear modulus applicable to an intrinsic process.

Because diffusion of uncharged particles requires no electrostatic energy, the activation energies of noble gases can be used to derive the doorway radius, which is then used as an input parameter for modelling the activation energy of charged particles. The doorway radius can be determined from a plot $\sqrt{E_a}$ vs. r at the intercept $\sqrt{E_a} = 0$ and is not dependent on the equation (Eqns. 4 to 7) used or other parameters such as G or λ.

It is evident that the calculated doorway radii depend on the choice of the noble gas atomic diameter used. Available data from the literature exhibit a significant scattering (cf. Zhang and Xu, 1995), and it is not clear what diameter is appropriate for condensed matter. It is a prerequisite using a reasonable set of noble gas diameters because the derived doorway radius is an input parameter for calculating the activation energies of charged particles. The doorway radius should be in the range of the observed minimum in the activation energies (i.e., around 1 Å). This follows from Eqns. 9 and 11, where the minimum is defined by the contribution of the elastic part.

With this assumption, we evaluate the data sets of Dushman (1949), Hirschfelder et al. (1954), Pauling (1960), Bondi (1964), Ozima and Podosek (1983), and Zhang and Xu (1995). Only the atomic diameters given by Hirschfelder et al. (1954), Pauling (1960), and Bondi (1964) yield doorways within the range of ~1 Å. Because the best fit is obtained employing the data of Hirschfelder et al. (1954), we used this data set for the calculation of the doorway radii and for the parameterization of the models. The doorway radius for SiO_2, $NaAlSi_3O_8$, and $NaAlSi_2O_6$, calculated from the mean values of all available data, are summarized in Table 8. The E_f term is ignored in this calculation because this yields doorway radii significantly greater than 1 Å. The activation energies for He and Ne in albite glass (Roselieb et al., 1992) are too high (Fig. 10) when compared with the trend in silica (Fig. 9) or jadeite (Fig. 11), so we did not use these values for the following calculations. Instead, we included the activation energy of permeation for He in albite and jadeite glass (Shelby and Eagan, 1976).

4.3. Calculation of Activation Energies of Diffusion

Now the unknown parameters are reduced to the jump distance λ, the dielectric constant ε, and the energy of formation E_f. Fitting these parameters with the models (Eqns. 9 and 11) yields for the modified Anderson-Stuart model (Eqn. 9) negative E_f values (approximately -15 to -45 kJ/mol) and for the model developed here (Eqn. 11) positive values (between 17 and 23 kJ/mol), but with large errors up to 100%. Although the standard deviation between measured and calculated values is reduced by 3 to 10% if E_f is ignored, we fitted both equations (Eqns. 9 and 11) only with λ and ε and set $E_f = 0$ because the E_f values do not allow a meaningful comparison of both models. The standard deviation between measured and calculated values is somewhat better (7 to 18%) when Eqn. 9 is used. The results for all parameters are summarized in Table 8, and the experimental data are compared with the calculated activation energies using Eqns. 9 and 11 in Figures 9 to 11 for silica, albite, and jadeite composition.

If G as input parameter is varied by $\pm 10\%$, the fitted values for λ and ε change as well by $\pm 10\%$, whereas the standard deviation between measured and calculated activation energies varies by $\pm 3\%$. The doorway radius is estimated with large errors of approximately ± 0.3 Å (Table 8). Consequently, the fitted parameters are significantly influenced by r_d, specifically ε up to 40% and λ up to a factor of two. However, the derived r_d values are reasonable because they agree with the observed minimum in Figures 9 to 11. In general, there is very good agreement between measured and calculated activation energies, demonstrating that both models are reasonable. The experimentally observed minimum for Na, and Ca and Sr are particularly well reproduced by the fit to both equations. The 1σ standard deviation between the measured and calculated values ranges between 23 and 35 kJ/mol (cf. Table 8) and is somewhat larger than the range of the experimental error.

From Table 8 and Figures 9 to 11, it is evident that the standard deviation for the charged particles is poorest for the alkalies in vitreous albite; this is possibly caused by different starting materials. It should be mentioned that a much better fit is produced if the activation energies determined from Jambon and Delbove (1976) for Rb and Cs are used, which are derived from experiments at 4 kbar but with the same starting material as used for the investigation of Li, Na, and K at 1 bar (Jambon and Carron, 1976; Jambon and Semet, 1978).

5. DISCUSSION OF FITTED PARAMETERS

As the best fit to the experimental data is obtained with the modified Anderson-Stuart model (Eqn. 9), we briefly discuss the derived fit parameters employing this equation.

5.1. Dielectric Constant

The dielectric properties of the compositions considered here are well known only for silica glass. If network-modifying cations are introduced into SiO_2, the dielectric constant increases depending on the field strength (e.g., Scholze, 1988). The best fit of the experimentally determined activation energies employing Eqn. 9 yields dielectric constants of 5.3 for SiO_2, 7.9 for $NaAlSi_3O_8$, and 8.7 for $NaAlSi_2O_6$ (Table 8). The experimentally derived dielectric constant for SiO_2 is ~4 over a wide range of frequency (Bansal and Doremus, 1986). To our knowledge, no experimentally determined dielectric constants are available for $NaAlSi_3O_8$ and $NaAlSi_2O_6$ at a sufficiently high frequency. However, the dielectric constants can be calculated from molar quantities by using the data of Appen and Bresker (1952), yielding values of 6.2 and 7 for $NaAlSi_3O_8$ and $NaAlSi_2O_6$, respectively. These data from the literature are in reasonable agreement with the fitted parameters. Specifically, the increase in the dielectric constant from SiO_2 to $NaAlSi_3O_8$ and $NaAlSi_2O_6$ of ~1.5 is well represented by the obtained parameters.

5.2. Jump Distances

The derived jump distances in isostructural compositions of SiO_2, $NaAlSi_3O_8$, and $NaAlSi_2O_6$ vary between 10 and 12 Å (cf. Table 8) and agree within error. These values can be compared with other known interatomic distances in vitreous phases of the system SiO_2-$NaAlSi_2O_6$. Generally the derived jump distances appear to be large when compared with the O-Si-O-distance of, for example, 3.26 Å for albite glass (Taylor and Brown, 1979) or the Na-O-distance of 2.62 Å in isostructural nepheline glass (McKeown et al., 1985). Direct information on the environment of noble gases in these structures is available from the XAS measurements of Wulf et al. (1999). They investigated the local neighbours of Kr incorporated in supercooled SiO_2 melt and found Kr-O distances of 3.45 Å. Because the structure of glasses and melts along the join SiO_2-$NaAlSi_2O_6$ is described as tridymite-like (Taylor and Brown, 1979), a comparison to the interatomic distances of 4 Å in crystalline tridymite is possible. Evidence for jump lengths greater than 10 Å stems from the structural analysis of gas diffusion by means of statistical mechanics and two-dimensional Zachariasen schematics (Shackelford, 1982). Shackelford (1982) estimated jump lengths between 8 and 23 Å for noble gases in vitreous silica. Roselieb et al. (1996) applied the equation of McElfresh and Howitt (1986) to interpret the activation volumes of Ar and Kr diffusion in supercooled jadeite melt and derived an average jump distance of 18 Å. Shackelford (1982) discussed possibilities to explain such large jump distances inter alia the existence of network channels. Such percolation channels were proposed by Greaves (1985) and Greaves et al. (1991) in their modified random network model. Herein, network-modifying cations in simple Na-silica glasses are enriched in network channels, thus enhancing the alkali mobility. Direct evidence about distances between the network modifiers is available from X-ray and neutron scattering experiments, and these range from 6 to 8 Å (cf. Brown et al., 1995). Although there is some evidence for jump distances larger than a few angstroms, the derived jump distances should be considered with great care. Direct probing of the interatomic distances would be a valuable contribution, improving the modeling of activation energies for diffusion in vitreous silicates.

5.3. Doorway Radius

The doorway radii of $\sim$1 Å determined in the system SiO_2-$NaAlSi_2O_6$ agree within error ($\pm$0.3 Å), which seems reasonable in view of the structural similarity (see above; Taylor and Brown, 1979; Walter et al., 2000). However, there is some evidence from Raman spectroscopy (Seifert et al., 1982) and molecular dynamic simulation (Dempsey and Kawamura, 1984) that smaller ring structures with increasing substitution of Si by (Na + Al) occur. Moreover, the radial distribution analysis of Taylor and Brown (1979) indicates decreasing structural order with increasing (Na + Al) content. Therefore, one could expect that with increasing substitution of Si by (Na + Al), a smaller doorway radius appears. However, this decrease is possibly within the experimental error, and further investigations, especially of He and Ne diffusion in $NaAlSi_3O_8$ and $NaAlSi_2O_6$, would be helpful to resolve this problem. This would also be helpful to better constrain the value for E_f.

6. CONCLUSIONS

Tracer diffusivities of alkaline earth cations measured by electron microprobe were found to be comparable to diffusivities measured at infinite dilution. Only Mg, and possibly other elements with high charge/size ratio, exhibits a dependence on concentration.

With changing composition of the matrix, especially substitution of Si by (Na + Al) along the join SiO_2-$NaAlSi_2O_6$, diffusivities of alkaline earths increase and activation energies decrease.

The low diffusivity of Mg is a new and important piece of information. Even though Mg diffusivity was measured at infinite dilution, it clearly appears that Mg, despite its small ionic radius, is not a fast-diffusing cation in silicate melts. Because Mg is an abundant element in natural systems, understanding the effects on crystal dissolution and growth, exchange with impurities, etc., that may be under the control of diffusion should take into account the particular behavior of Mg.

The modified Anderson-Stuart model represents activation energies reasonably well. The parameters obtained for the jump distance λ and the dielectric constant ε are in reasonable agreement with values from other estimates in the literature. The structural parameter λ varies marginally from one composition to the next, in accordance with the structural similarity along the join SiO_2-$NaAlSi_2O_6$. The dependence of the dielectric constant on composition compares well with values calculated for bulk compositions. The least-square residuals are comparable to the observed analytical uncertainties. An alternative formulation concerning the electrostatic contribution in the Anderson-Stuart model as quadratic on the charge z yields somewhat poorer least-squares residuals. The fitted parameters for λ are comparable with those derived from the Anderson-Stuart model, while the dielectric constants are lower.

Further applications of both models to other silicate melts and glasses with additional measurements for trivalent cations such as rare earth elements, Ga, and Al are urgently needed to further test the models on other melt compositions and to further extrapolate both models to highly charged cations. This would also be helpful in deciding which model is more appropriate and whether bulk properties such as dielectric constants can be used, or if they depend on charge and size of the diffusing cation.

In conclusion, modeling the activation energy of diffusion in melts of noble gases, alkalies, and alkaline earths as rigid spheres in a solid medium seems to be successful.

Acknowledgments—K.R. gratefully acknowledges support by the EC (HCM fellowship). We thank D. Badia, E. Delairis, A. Hampe, P. Meier, and K. Sander for technical assistance. T. Heinrichs helped with the access to the scanning electron microscope to find out improvements of the Mg pretreatment. During microprobe analyses, we benefited from the help of the CAMPARIS team. D. Dingwell kindly fabricated the albite glass. Steve Foley and Sharon Webb improved the manuscript with helpful comments. Y. Liang, F. Ryerson, and two anonymous reviewers provided useful reviews.

Associate editor: F. J. Ryerson

REFERENCES

Albarède F. and Bottinga Y. (1972) Kinetic disequilibrium in trace element partitioning between phenocrysts and host lava. *Geochim. Cosmochim. Acta* **36,** 141–156.

Anderson O. L. and Stuart D. A. (1954) Calculation of activation energy of ionic conductivity in silica glasses by classical methods. *J. Am. Ceram. Soc.* **37,** 573–580.

Appen A. A. and Bresker R. I. (1952) Abhängigkeit der Dielektrizitätskonstante und des Verlustwinkels von Silikatgläsern von ihrer Zusammensetzung. *J. Tech. Phys. USSR* **22,** 946–954.

Bansal N. P. and Doremus R. H. (1986) *Handbook of Glass Properties*. Academic Press.

Blundy J. and Wood B. (1994) Prediction of crystal-melt partition coefficient from elastic moduli. *Nature* **372,** 452–454.

Bondi A. (1964) Van der Waals volumen and radii. *J. Phys. Chem.* **68,** 441–451.

Brown G. E., Farges F., and Calas G. (1995) X-ray scattering and X-ray spectroscopy studies of silicate melts. In: Structure, dynamics and properties of silicate melts (eds. Stebbins J. F., McMillan P. F., and Dingwell D. B.). *Rev. Mineral.* **32**, 317–410.

Carroll M. R. (1991) Diffusion of Ar in rhyolite, orthoclase and albite composition glass. *Earth Planet. Sci. Lett.* **103,** 156–168.

Carroll M. R. and Stolper E. M. (1991) Argon solubility and diffusion in silica glass: Implications for the solution behavior of molecular gases. *Geochim. Cosmochim. Acta* **55,** 211–225.

Carroll M. R., Sutton S. R., Rivers M. L., and Woolum D. (1993) An experimental study of Krypton diffusion and solubility in silicic glasses. *Chem. Geol.* **109,** 9–28.

Carron J. P. (1969) Recherches sur la viscosite et les phenomenes de transport des ions alcalins dans les obsidiennes granitiques. Ph.D. thesis. University of Paris.

Chakraborty S., Farver J. R., Yund R. A., and Rubie D. C. (1994) Mg tracer diffusion in synthetic forsterite and San Carlos olivine as a function of P, T and f_{O_2}. *Phys. Chem. Minerals* **21,** 489–500.

Crank J. (1975) *The Mathematics of Diffusion.* 2nd. ed. Clarendon.

Dempsey M. J. and Kawamura K. (1984) Molecular dynamics simulation of the structure of aluminosilicate melts. *Natl. Environ. Res. Council Ser D* **25,** 49–56.

Dingwell D. and Webb S. (1989) Structural relaxation in silicate melts and non-newtonian melt rheology in geologic processes. *Phys. Chem. Minerals* **16,** 508–516.

Doremus R. H. (1969) Electrical conductivity and electrolysis of alkali ions in silica glass. *Phys. Chem. Glasses* **10,** 28–33.

Dushman S. (1949) *Scientific Foundations of Vacuum Technique*. Wiley.

Frank R. C., Swets D. E., and Lee R. W. (1961) Diffusion of neon isotopes in fused quartz. *J. Chem. Phys.* **35,** 1451–1459.

Frenkel J. (1946) *Kinetic Theory of Liquids*. Oxford University Press.

Frischat G. H. (1970) Natriumdiffusion in verschiedenen Kieselgläsern. *Glastechn. Ber.* **43,** 482–488.

Fritzsche T. (1990) Impedanzmessungen an Gläsern des Systems Albit-Nephelin im Glastransformations-Bereich. Ph.D. thesis. University of Göttingen.

Fuchser D. (1996) Impedanzspektroskopische und kalorimetrische Untersuchungen an silikatischen Gläsern. Klaus Bielefeld Verlag. Friedland. Ph.D. thesis. University of Göttingen.

Greaves G. N. (1985) EXAFS and the structure of glass. *J. Non-Cryst. Solids* **71,** 203–217.

Greaves G. N., Gurman S. J., Catlows C. R. A., Chadwick A. V., Houde-Walter S., Henderson C. M. B., and Dobson B. R. (1991) A structural basic for ionic diffusion in oxide glasses. *Phil. Mag. A* **64,** 1059–1072.

Hirschfelder J. O., Curtiss C. F., and Bird R. B. (1954) *Molecular Theory of Gases and Liquids*. Wiley.

Hofmann A. W. and Hart S. R. (1978) An assessment of local and regional isotopic equilibrium in the mantle. *Earth Planet. Sci. Lett.* **38,** 44–62.

Jambon A. (1980) Diffusion cationique dans les silicates fondus: Étude expérimentale et modèles pétrologiques. Ph.D. thesis. Université d'Orléans.

Jambon A. (1982) Tracer diffusion in granitic melts: Experimental results for Na, K, Rb, Cs, Ca, Sr, Ba, Ce, Eu to 1300°C and a model of calculation. *J. Geophys. Res.* **87(B13),** 10797–10810.

Jambon A. (1983) Diffusion dans les silicates fondus: Un bilan des connaissances actuelles. *Bull. Mineral.* **106,** 229–246.

Jambon A. and Carron J.-P. (1976) Diffusion of Na, K, Rb and Cs in glasses of albite and orthoclase composition. *Geochim. Cosmochim. Acta* **40,** 897–903.

Jambon A. and Delbove F. (1976) Effet d'une pression de 4 kbar sur la diffusion de Rb et Cs dans des verres d'albite et d'orthose. *C. R. Acad. Sci. D* **282,** 949–952.

Jambon A. and Delbove F. (1977) Étude à 1 bar, entre 600 et 1100°C, de la diffusion du calcium dans les verres feldspathiques. *C. R. Acad. Sci. Paris Ser. D* **284,** 2191–2194.

Jambon A. and Semet M. P. (1978) Lithium diffusion in silicate glasses of albite, orthoclase and obsidian composition: An ion-microprobe determination. *Earth Planet. Sci. Lett.* **37,** 445–450.

McElfresh D. K. and Howitt D. G. (1986) Activation enthalpy for diffusion in glass. *J. Am. Ceram. Soc.* **69,** C237–C238.

McKeown D. A., Waychunas G. A., and Brown G. E. Jr. (1985) EXAFS and XANES study of the local coordination environment of sodium in a series of silica-rich glasses and selected minerals within the Na_2O-Al_2O_3-SiO_2 system. *J. Non-Cryst. Solids* **74,** 325–348.

Nakayama G. S. and Shackelford J. F. (1990) Solubility and diffusivity of argon in vitreous silica. *J. Non-Cryst. Solids* **126,** 249–254.

Ozima M. and Podosek F. (1983) *Noble Gas Geochemistry*. Cambridge University Press.

Pauling L. (1960) *The Nature of the Chemical Bond*. 3rd ed. Cornell University Press.

Perkins W. G. and Begeal D. R. (1971) Diffusion and permeation of He, Ne, Ar, Kr and D_2 through silicon oxide thin films. *J. Chem. Phys.* **54,** 1683–1694.

Roselieb K., Rammensee W., Büttner H., and Rosenhauer M. (1992) Solubility and diffusion of noble gases in vitreous albite. *Chem. Geol.* **96,** 241–266.

Roselieb K., Rammensee W., Büttner H., and Rosenhauer M. (1995) Diffusion of noble gases in melts of the system SiO_2-$NaAlSi_2O_6$. *Chem. Geol.* **120,** 1–13.

Roselieb K., Büttner H., Eicke U., Köhler U., and Rosenhauer M. (1996) Pressure dependence of Ar und Kr diffusion in a jadeite melt. *Chem. Geol.* **128,** 207–216.

Roselieb K. and Jambon A. (1997) Tracer diffusion of K, Rb and Cs in a supercooled jadeite melt. *Geochim. Cosmochim. Acta* **61,** 3101–3110.

Roselieb K., Chaussidon M., Mangin D., and Jambon A. (1998) Lithium diffusion in vitreous jadeite ($NaAlSi_2O_6$): An ion microprobe investigation. *Neues Jahrb. Mineral.* **172,** 245–247.

Rothman S. J., Marcuso T. L. M., Nowicki L. J., Baldo P. M., and McCormick A. W. (1982) Diffusion of alkali ions in vitreous silica. *J. Am. Ceram. Soc.* **65,** 578–582.

Scholze H. (1988) *Glas: Natur, Struktur und Eigenschaften.* Springer-Verlag.

Seifert F. A., Mysen B. O., and Virgo D. (1982) Three-dimensional network structure of quenched melts (glass) in the system SiO_2-$NaAlO_2$, SiO_2-$CaAl_2O_4$, and SiO_2-$MgAl_2O_4$. *Am. Mineral.* **67,** 696–717.

Shackelford J. F. (1982) A gas probe analysis of structure in bulk and surface layers of vitreous silica. *J. Non-Cryst. Solids* **49,** 299–307.

Shannon R. D. (1976) Revised effective radii and systematic studies of interatomic distances in halides and chalcogenides. *Acta Cryst.* **A32**, 751–767.

Shelby J. E. (1971) Temperature dependence of He diffusion in vitreous silica. *J. Am. Ceram. Soc.* **54,** 125–126.

Shelby J. E. (1972) Helium migration in glass-forming oxides. *J. Appl. Phys.* **43,** 3068–3072.

Shelby J. E. and Eagan R. J. (1976) Helium migration in sodium aluminosilicate glasses. *J. Am. Ceram. Soc.* **59,** 420–425.

Siewert R. and Rosenhauer M. (1994) Light scattering in jadeite melt: Strain relaxation measurements by photon correlation spectroscopy. *Phys. Chem. Minerals* **21,** 18–23.

Siewert R. and Rosenhauer M. (1997) Viscoelastic relaxation measure-

ments in the system SiO_2-$NaAlSiO_4$ by photon correlation spectroscopy. *Am. Mineral.* **82,** 1063–1072.

Swets D. E., Lee R. W., and Frank R. C. (1961) Diffusivity of helium in fused quartz. *J. Chem. Phys.* **34,** 17–22.

Taylor M. and Brown G. E. (1979) Structure of mineral glasses. II. The SiO_2-$NaAlSiO_4$ join. *Geochim. Cosmochim. Acta* **43,** 61–75.

Walter H., Büttner H., Roselieb K., and Rosenhauer M. (2000) Pressure dependence of the solubility of Ar and Kr in melts of the system SiO_2-$NaAlSi_2O_6$. *Am. Mineral.* **85,** 1117–1127.

Wei G. C. T. and Wuensch B. J. (1976) Tracer concentration gradients for diffusivities exponentially dependent on concentration. *J. Am. Ceram. Soc.* **59,** 295–299.

Wortman R. S. and Shackelford J. F. (1990) Gas transport in vitreous silica fibers. *J. Non-Cryst. Solids* **125,** 280–286.

Wulf R., Calas G., Ramos A., Büttner H., Roselieb K., and Rosenhauer M. (1999) Structural environment of krypton dissolved in vitreous silica. *Am. Mineral.* **84,** 1461–1463.

Zhabrev V. A., Moiseev V. V., Sviridov S. I., and Chistoserdov V. G. (1976) Diffusion of divalent ions in vitreous silica. *Soviet J. Glass Phys. Chem.* **2,** 326–329.

Zhang Y. and Xu Z. (1995) Atomic radii of noble gas elements in condensed phases. *Am. Mineral.* **80,** 670–675.

Zhang Y., Walker D., and Lesher C. E. (1989) Diffusive crystal dissolution. *Contrib. Mineral. Petrol.* **102,** 492–513.